Control of bursting by local inhibition in the rat subiculum *in vitro*

L. Menendez de la Prida

Departamento de Neurobiología-Investigación, Hospital Ramón y Cajal, Ctra Colmenar Km 9, Madrid 28034, Spain

The subiculum, which provides the major hippocampal output, contains different cell types including weak/strong bursting and regular-spiking cells, and fast-spiking interneurons. These cellular populations play different roles in the generation of physiological rhythms and epileptiform activity. However, their intrinsic connectivity and the synaptic regulation of their discharge patterns remain unknown. In the present study, the local synaptic responses of subicular cell types were examined *in vitro*. To this purpose, slices were prepared at a specific orientation that permitted the antidromic activation of projection cells as a tool to examine local circuits. Patch recordings in cell-attached and whole-cell configurations were combined with neurobiotin labelling to classify cell types. Strong (~75 %), but not weak (~22 %), bursting cells typically fired bursts in response to local synaptic excitation, whereas the majority of regular-spiking cells (~87 %) remained silent. Local excitation evoked single spikes in more than 70 % of fast-spiking interneurons. This different responsiveness was determined by intrinsic membrane properties and not by the amplitude and pharmacology of synaptic currents. Inhibitory GABAergic responses were also detected in some cells, typically as a component of an excitatory/inhibitory sequence. A positive correlation between the latency of the excitatory and inhibitory responses, together with the glutamatergic control (via non-NMDA receptors) of inhibition, suggested a local mechanism. The effect of local inhibition on synaptically activated firing of different cell types was evaluated. It is shown that projection bursting cells of the subiculum are strongly controlled by local inhibitory circuits.

The subiculum provides the major output of the hippocampus, but it also receives abundant projections from many cortical and subcortical regions (Van Groen & Lopes da Silva, 1986; Naber & Witter, 1998; Ishizuka, 2001). One important feature of the subicular responses to afferent stimulation is the activation of local inhibitory circuits through a feedforward mechanism (Finch & Babb, 1980; Colino & De Molina, 1986; Finch *et al.* 1988; Behr *et al.* 1998). This typically consists of an EPSP–IPSP sequence that results in firing suppression. However, although this local inhibition plays a fundamental role in shaping responses to incoming inputs (Alger & Nicoll, 1982; Buszaki, 1984), the underlying cellular mechanisms in the subiculum remain unexplored.

The subiculum contains different cellular types including bursting and non-bursting projection cells (Mason, 1993; Stewart & Wong, 1993) and a variety of GABAergic interneurons (Kawaguchi & Hama, 1987; Menendez de la Prida *et al.* 2003). Subicular bursting neurons constitute an important cell group for the generation of gamma oscillations (Stanford *et al.* 1998) and epileptiform activity (Harris & Stewart, 2001; Cohen *et al.* 2002). Although the basic intrinsic connectivity of the subiculum has been identified, some issues need to be clarified. For example, it is unknown whether bursting and non-bursting neurons differentially respond to local excitation, even though the bursting nature of the subiculum is widely accepted. Similarly, little is known about the local inhibitory control of bursting cells. This is especially important since local inhibition could play a role in controlling cellular excitability (Miles & Wong, 1987). Recently, the spontaneous activity from the subiculum obtained from temporal lobe epileptic patients was studied *in vitro* (Cohen *et al.* 2002). It was shown that interictal-like activity, which was confined to this structure, was mediated by altered GABAergic responses. Thus, the properties of subicular inhibitory circuits may significantly regulate the operation of this structure under normal and pathological situations.

The goal of the present work was to identify the responses of different subicular cell types to local excitation and to quantify the effect of inhibition on these firing patterns. Local synaptic responses were examined in isolation by preparing slices at a specific orientation that assured an exclusively antidromic activation of projection cells.

Antidromic spikes in some projection cells were used to examine the evoked synaptic responses in other cells (Miles & Wong, 1986). Patch recordings in both cell-attached and whole-cell configurations were combined with extracellular recordings in order to characterize cell responses before and after a disruption of the intracellular medium. I found that responses to local glutamatergic excitation depended on the electrophysiological cell types (i.e. bursting, non-bursting and fast-spiking (FS) cells), with bursting cells being separated into two groups. Local GABAergic circuits were typically activated concomitantly with glutamatergic excitation. I found that bursting cells, which are the major contributors to local levels of activity in the subiculum, are under the control of GABAergic inhibition. This suggests that the normal operation of the subiculum is strongly regulated by local inhibitory circuits.

METHODS

Slice preparation

Juvenile Wistar rats (17–20 days old) were anaesthetized with ether and decapitated in accordance with European guidelines (86/609/EEC). The brain was immediately removed, and chilled in 4 °C oxygenated (95 % O_2–5 % CO_2) artificial cerebrospinal fluid (ASCF: 125 mM NaCl, 3 mM KCl, 1 mM $MgCl_2$, 1.2 mM NaH_2PO_4, 2 mM $CaCl_2$, 22 mM $NaHCO_3$, 10 mM glucose). Brain slices (350 μm) at an orientation that would permit antidromic activation of subicular projection cells were prepared using a vibratome. To this purpose, the dorsal part of the brain was glued to an agar ramp of 8–10 deg, with the caudal end of the brain facing the blade. After sectioning, slices were maintained in ACSF at room temperature for at least 1 h before being transferred to a submerged-type recording chamber (flow rate of 1–1.5 ml min^{-1} at 32–34 °C) attached to an Olympus microscope. Once in the recording chamber, the precise orientation of fibre tracts in slices was tested by stimulating both the subicular alveus and the CA1 stratum pyramidale, while recording field potentials in the subiculum (see first section of Results). Since the purpose of this study was to examine the antidromically activated synaptic responses, those slices showing CA1-evoked orthodromic population spikes were not accepted.

Extracellular recordings and stimulation

Extracellular field recordings were made using patch-clamp pipettes filled with ACSF (tip resistance ~7 MΩ). Patch pipettes were made from borosilicate glass capillaries (outer diameter 1.2 mm; inner diameter 0.69 mm, Harvard Apparatus). Signals were amplified and band-pass filtered at 0.1 Hz–100 kHz. Monopolar stimulation was delivered via tungsten electrodes (tip diameter 10–20 μm, World Precision Instruments). Stimulation consisted of square-wave pulses of 0.1 ms duration and 0.5–1 mA amplitude. The position of the stimulating and the recording electrodes were set at the beginning of each experiment by maximizing the antidromic population spike (1–1.5 mV) at a specific stimulation strength, which was comparable in all slices (coefficient of variation of the stimulation strength: 0.16, data from n = 15 slices).

Patch recordings

Somatic patch-clamp recordings were made under visual control (× 60 immersion lens) using an Axoclamp 2B amplifier (Axon Instruments), digitized (Digidata 1322A, Axon Instruments) and

stored on disk at a sampling frequency of 10 kHz. Patch pipettes were filled with intracellular solution containing (mM): 131 potassium gluconate, 6 KCl, 1 $MgCl_2$, 1 NaCl, 1 EGTA, 5 Hepes, 2 K_2 ATP, 0.3 NaGTP, pH 7.3 adjusted with KOH and osmolarity between 290 and 300 mosmol l^{-1}. For some voltage-clamp experiments, the following solution was also used (mM): 115 caesium gluconate, 4 $MgCl_2$, 1 EGTA, 5 Hepes, 2 Na_2 ATP, 0.3 Na GTP, pH 7.3 adjusted with CsOH and osmolarity between 290 and 300 mosmol l^{-1}. For subsequent morphological analysis, 0.1–0.5 % neurobiotin (Vector Laboratories, Burlingame, CA, USA) was added to the internal solution. Patch pipettes had a resistance of 4–6 MΩ. Capacitance compensation and bridge balance were performed. The junction potentials (~7 mV for K-based solution and ~1 mV for Cs-based solution) were not corrected.

Patch recordings were performed using cell-attached and whole-cell configurations in current-clamp and voltage-clamp modes. Once in the cell-attached configuration, cell responses to antidromically activated synaptic excitation were recorded. The seal was then ruptured and the whole-cell configuration in current-clamp mode was established. The intrinsic firing pattern and membrane properties (resting membrane potential (RMP), input resistance and firing threshold) were immediately tested. Cells were classified electrophysiologically as weak (IB−) or strong (IB+) bursting, regular-spiking (RS) or FS, from their responses to depolarizing current pulses of 500 ms duration (Stewart & Wong, 1993; Staff *et al.* 2000; Menendez de la Prida *et al.* 2003). Bursting cells firing only one burst in response to depolarizing current pulses were classified as IB− cells, whereas those bursting cells that fired more than one burst were classified as IB+.

Evoked synaptic activity was examined in both current- and voltage-clamp modes at different membrane potentials between −50 and −85 mV. In some experiments the Cs-based internal solution was used for estimating synaptic currents. The pharmacological nature of synaptic activity was tested using the glutamatergic receptor antagonists 6-cyano-7-nitroquinoxaline-2,3-dione (CNQX) and DL-2-amino-5-phosphonopentanoic acid (AP5), and the GABA$_A$ receptor antagonist picrotoxin (PTX). All drugs were purchased from Sigma.

Local application of high [K$^+$] and glutamate

In some experiments, the effect of local application of high [K$^+$] and glutamate was evaluated. The properties of local excitatory circuits can be studied using this approach (Christian & Dudek, 1988). To this purpose, a pressure-ejection system (General Valve) was connected to a patch pipette filled with a solution of either 145 mM KCl or 0.5 mM L-glutamate monosodium salt. Neutral red (1 %; Sigma) was initially used to adjust pressure (20 p.s.i. (130 kPa)) and duration (5–10 ms) so that a region of 50–100 μm radius would be perfused.

Morphological identification and measurements

Neurons loaded with neurobiotin were processed for morphological analysis. After the experiment, the slice was fixed overnight in 4 % paraformaldehyde in PBS (0.1 M, pH 7.4). After pretreatment with H_2O_2 (0.3 %) and Triton X-100 (0.6 %), slices were processed by incubation in a 1:100 dilution of an avidin-biotin-peroxidase complex kit (Vector Laboratories) over a 3 h period. Visualization was performed using a solution of 0.03 % 3,3-diaminobenzidine and 0.005 % H_2O_2. The reaction was followed under visual control and stopped after 5–10 min depending on labelling intensity. The slices were washed in Tris-buffered saline (0.5 M) and mounted on gelatin-coated glass slides using glycerol (50 % in Tris-buffered

saline) and Eukitt mounting medium (Fluka). More than 60 % of neurobiotin-filled cells were successfully recovered. A group of these cells were drawn with the aid of × 40 and × 60 objectives and a camera lucida attachment. The length of the main axon collateral was measured from the camera lucida drawings using a magnetic tablet (SummaSketch III) and the Scion image analysis program (Scion). The position of the stimulation electrode was recognized in some slices as a lesion in the subicular alveus.

Data measurements and analysis

Intrinsic membrane properties were measured using current steps in the whole-cell current-clamp mode. Input resistance was determined from cell responses to hyperpolarizing current pulses of 500 ms duration. To determine firing threshold, depolarizing pulses of 50 ms were used. Firing threshold was defined at the inflexion point of the voltage trace. For comparison between different cell types, the amplitude and half-duration of the excitatory synaptic events was determined in both current- and voltage-clamp mode at −65 mV. Inhibitory events were analysed at −50 and −55 mV. For the calculation of the latency of antidromic spikes, the time delay between the stimulus start and the onset of the antidromic spike was measured. All results are given as means ± S.D., with the number of cells (or slices) indicated in every case. Results were compared using Student's *t* test or ANOVA. The significance level is specified.
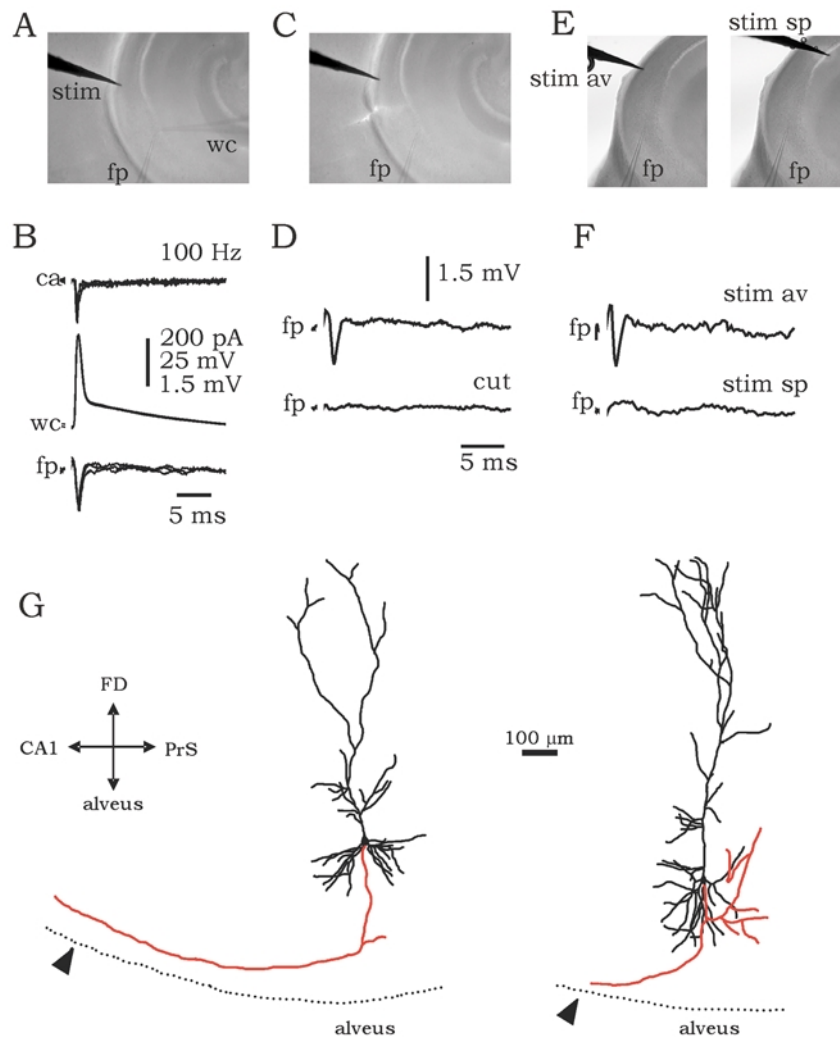
Figure 1. Antidromic activation of projection cells of the subiculum

A, hippocampal slices were prepared at an orientation that permitted antidromic but not orthodromic activation of subicular cells. The placement of the stimulating (stim), field potential (fp) and whole-cell (wc) electrodes is shown. *B*, simultaneous field and patch recordings in cell-attached (ca) and whole-cell configurations. Stimulation of the alveus at 100–150 Hz elicited antidromic spikes. *C*, in some slices a cut was performed at the subicular alveus to test the antidromic nature of the field recording (fp). *D*, field potential recordings before and after cutting the alveus. *E* and *F*, the precise orientation of fibre tracts was tested in slices by stimulating both the subicular alveus (av) and the CA1 stratum pyramidale (sp), whilst recording field potential in the subiculum. Scales are the same as in *D*. *G*, camera lucida reconstruction of projection cells of the subiculum showing the position of the stimulating electrode (arrowhead). Axon collaterals are shown in red. The orientation of the cells is shown by the axis on the left: FD (fascia dentata), PrS (pre-subiculum).

RESULTS

Antidromic activation of local excitatory circuits

The main axon collateral of projection cells from the subiculum travels through the alveus to project to other subcortical structures (Finch *et al.* 1983; Köhler, 1986). Slices were prepared (see Methods) so that a large proportion of these axons were present and the CA1 input to the subiculum was absent (Fig. 1*E*, *F*; also see Methods). Figure 1*B* shows how in these slices the extracellular stimulation of the alveus activated an antidromic population spike (fp). Simultaneous patch recordings in cell-attached (ca) and whole-cell (wc) current-clamp configurations revealed the properties of these antidromic spikes in a subpopulation of cells (*n* = 10; see Fig. 1*A* for electrode localization of the experiment shown in *B*).

Intracellularly, antidromic spikes were characterized by a constant latency (1.42 ± 0.43 ms, *n* = 6 cells) independent of the RMP and by a capacity to follow frequencies of 100–150 Hz. The antidromic population spike (latency: 1.14 ± 0.21 ms, *n* = 6 slices) was abolished by cutting the subicular alveus (*n* = 4 slices; Fig. 1*C*, *D*). The main axon collateral of four projection cells was successfully followed up to the putative stimulation site (visible as a mark in the tissue). The length of these axons was measured

(647 ± 233 μm; Fig. 1*G*) to estimate the axonal conduction velocity (0.59 ± 0.21 m s^{-1}).

Responsiveness of different cell types to local excitatory synapses

The responsiveness of different cell types was investigated using antidromic activation of projection cells. Cells were electrophysiologically classified in the whole-cell configuration as weak (IB−) or strong (IB+) bursting, RS or fast-spiking (FS), from their responses to depolarizing current pulses (see Methods). Anatomical examination of neurobiotin-loaded cells showed that the bursting and RS types were characteristic of projection cells and that FS cells corresponded to interneurons (Fig. 1*G* and Fig. 4, see also Menendez de la Prida *et al.* 2003). From a total of 85 cells, 18 were classified as IB−, 30 were IB+, 21 were RS and 16 cells were of the FS type. In order to characterize the responsiveness to local excitatory synapses, only those cells exhibiting pure EPSPs will be discussed initially (*n* = 60 cells). Antidromic spikes were not elicited in these cells, probably because axon collaterals were cut by the slicing procedure or did not pass near to the stimulation site.

In the cell-attached configuration, cells typically fired in three patterns in response to antidromic activation of projection cells: bursts, spikes and silent. The burst pattern
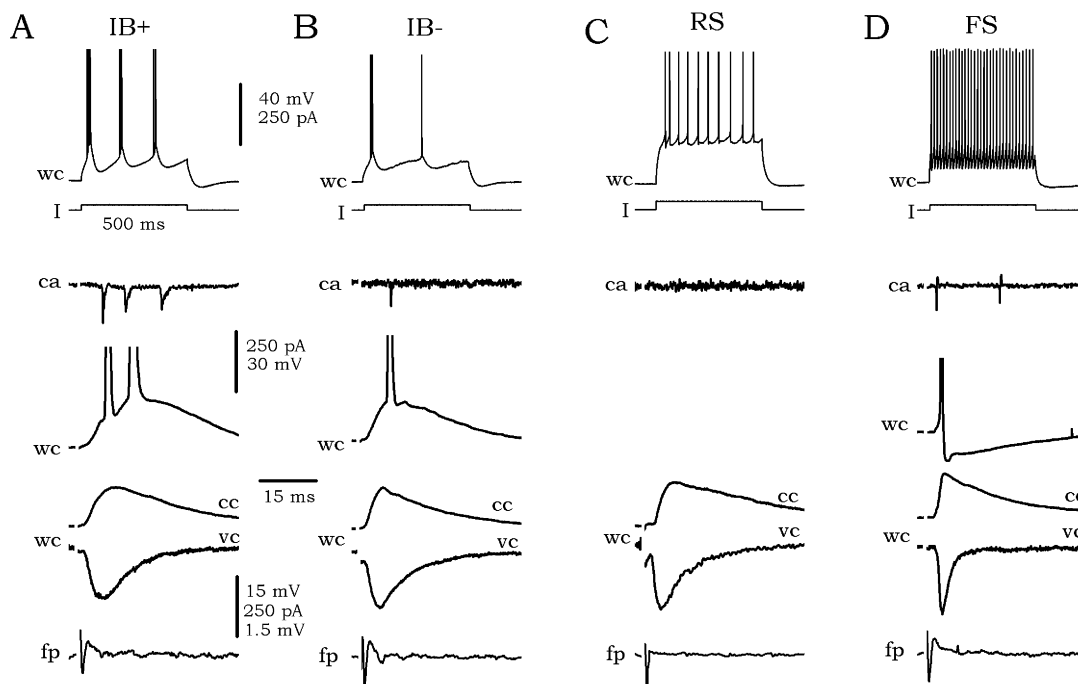
Figure 2. Responsiveness of different cell types to local excitation elicited by antidromic activation of projection cells

A, the typical firing pattern of strong bursting cells (IB+) in response to depolarizing current pulses (I) is shown at the top (wc trace). The response of this cell in cell-attached (ca) and whole-cell (wc) configurations to local excitation is shown below the I trace. The synaptic events were studied in both current- (cc) and voltage-clamp (vc) modes. Simultaneously recorded field potential (fp) is shown at the bottom. *B–D*, intrinsic and synaptic responses of weak bursting cells (IB−), regular-spiking cells (RS) and fast-spiking interneurons (FS).

Table 1. Properties of the EPSPs and EPSCs in different cell types

	IB+	IB−	RS	FS
Properties of EPSPs				
Amplitude - control (mV)	9.3 ± 3.9 (9)	6.3 ± 1.7 (8)	6.5 ± 3.2 (7)	8.4 ± 2.3 (7)
Amplitude - 100 μM AP5 (mV)	5.3 ± 2.4 (4)	3.9 ± 1.9 (4)	4.3 ± 2.7 (4)	6.8 ± 1.5 (4)
Amplitude - 10 μM CNQX (mV)	blocked (5)	blocked (4)	blocked (3)	blocked (3)
Half duration - control (ms)	25.5 ± 5.9 (9)	22.2 ± 4.6 (8)	25.5 ± 4.8 (7)	28.8 ± 3.9 (7)
Half duration - 100 μM AP5 (ms)	10.7 ± 3.1 (4)	12.3 ± 1.5 (4)	16.2 ± 5.3 (4)	14.7 ± 3.4 (4)
Properties of EPSCs				
Amplitude - control (nA)	204 ± 130 (9)	238 ± 103 (8)	191 ± 104 (7)	164 ± 75 (7)
Amplitude - 100 μM AP5 (nA)	164 ± 67 (4)	203 ± 53 (4)	135 ± 74 (4)	139 ± 53 (4)
Amplitude - 10 μM CNQX (nA)	blocked (5)	blocked (4)	blocked (3)	blocked (3)
Half duration - control (ms)	10.6 ± 2.9 (9)	7.9 ± 2.4 (8)	8.1 ± 1.9 (7)	8.9 ± 3.9 (4)
Half duration - 100 μM AP5 (ms)	6.8 ± 1.7 (4)	6.5 ± 1.9 (4)	5.9 ± 1.5 (4)	5.3 ± 1.3 (4)

The data are presented as means ± S.D. The number of cells is given in parentheses. AP5, DL-2-amino-5-phosphonopentanoic acid; CNQX, 6-cyano-7-nitroquinoxaline-2,3-dione, IB+, strong bursting cells; IB−, weak bursting cells; RS, regular-spiking cells; FS, fast-spiking cells.

Table 2. Intrinsic membrane properties of cells receiving local synaptic excitation

	IB+	IB−	RS	FS
RMP (mV)	−61.6 ± 1.7	−61.9 ± 2.9	−61.9 ± 4.5	−58.1 ± 3.8*
Input resistance (M Ω)	78 ± 28	74 ± 11	127 ± 37**	331 ± 153**
Firing threshold (mV)	13.7 ± 3.1	16.9 ± 3.2†	20.1 ± 5.9††	16.5 ± 3.9
n	12	18	15	15

In all cases, the asterisks indicating statistical significance are associated with the cell group that is statistically different. RMP, resting membrane potential. *RMP: FS cells *versus* other cell types, statistically different at $P < 0.05$. **Input resistance: RS and FS cells *versus* other cell types, statistically different at $P < 0.005$. †Firing threshold: IB+ *versus* IB−, statistically different at $P < 0.005$. ††Firing threshold: RS *versus* other cell types, statistically different at $P < 0.005$.

was typical of IB+ cells (9/12) and consisted of bursts of two to three spikes (Fig. 2*A*, trace ca). Once in the whole-cell configuration, synaptically activated bursts were also recorded at the RMP (−61.6 ± 1.7 mV, $n = 12$) and an EPSP, together with the corresponding synaptic current (EPSC), was evident under membrane hyperpolarization (−65 mV, Fig. 2*A*, traces wc). In contrast, IB− cells fired bursts (4/18) or single spikes (4/18; Fig. 2*B*, trace ca) in response to antidromically activated synaptic excitation at RMP (−61.9 ± 2.9 mV, $n = 18$), whereas more than half remained silent.

Antidromically activated synaptic excitation of RS cells typically did not induce firing (silent pattern; 13/15, Fig. 2*C*). In whole-cell recordings, evoked EPSPs and EPSCs were present at the RMP (−61.9 ± 4.5 mV, $n = 15$) without eliciting firing. On the contrary, the majority of FS cells (11/15, Fig. 2*D*) fired single spikes in the cell-attached and whole-cell configurations at RMP (−58.1 ± 3.8 mV, $n = 15$). Again, EPSPs and EPSCs were evident under membrane hyperpolarization of −65 mV.

Electrophysiological and pharmacological characterization of local EPSPs in different cell types

In order to understand these different responses, the electrophysiology and pharmacology of antidromically activated synaptic events was examined in 31 cells. The amplitudes and half-durations of evoked EPSPs and EPSCs were analysed. The stimulation strengths and the amplitudes of antidromic population spikes were comparable in all cases (see Methods).

There was no statistical difference in the amplitudes and half-durations of EPSPs and EPSCs between different cell types (Table 1). Evoked EPSPs were mainly dependent on non-NMDA receptors, since they were blocked by 10 μM CNQX but not by 100 μM AP5 (Table 1). The NMDA contribution to EPSCs was similar in all cell types (Table 1).

Different responsiveness is determined by intrinsic membrane properties and not by the amplitude of synaptic inputs

Different responses to synaptic excitation might also depend on intrinsic membrane properties. To explore this alternative, the RMPs, input resistances and firing thresholds of cells that received EPSPs ($n = 60$) were analysed. These results are summarized in Table 2.

FS interneurons exhibited the lowest RMP ($P < 0.05$) and a higher input resistance ($P < 0.005$) than projection cells. FS cells also had a lower firing threshold compared with RS

Table 3. Intrinsic and synaptic properties of firing versus non-firing projection cells

	Burst	Spikes	Silent
RMP (mV)	-60.8 ± 1.8 (13)	-62.6 ± 2.6 (7)	-62.3 ± 3.9 (25)
Input resistance (MΩ)	77 ± 28 (13)	85 ± 46 (7)	100 ± 34 (25)
EPSC amplitude K-solution (pA)	234 ± 109 (11)	296 ± 125 (6)	205 ± 86 (16)
EPSC amplitude Cs-solution (pA)	208 ± 37 (4)	197 ± 69 (4)	175 ± 50 (6)
Firing threshold (mV)	12.9 ± 1.8 (13)**	17.4 ± 3.4 (7)	19.2 ± 4.9 (25)

The number of cells is given in parenthesis. The asterisks indicating statistical significance are associated with the cell group that is statistically different. **Firing threshold, comparison between cell types at $P < 0.005$.

($P < 0.05$), but not compared with IB+ and IB− cells. This suggests that the higher probability of FS cells to fire spikes upon synaptic excitation depends on their intrinsic membrane properties (RMP, input resistance and firing threshold). However, the projection cells examined ($n = 45$) did not exhibit differences in RMP (Table 2). RS cells had a significantly higher input resistance than IB+ and IB− cells ($P < 0.005$), but their firing threshold was also higher. However, RS cells exhibited the lowest firing probability in response to synaptic excitation (only two cells out of 15 were induced to fire). Interestingly, IB+ cells, which typically fired bursts in response to synaptic excitation, had a lower firing threshold than IB− cells ($P < 0.005$), but their input resistance was similar. It is therefore likely that in contrast to FS interneurons, the RMP and input resistance do not determine the firing probability of projection cells of the subiculum, which seems rather to depend on the cellular firing threshold.

To further explore this possibility, data from projection cells ($n = 45$) were divided into three groups according to their pattern of synaptic activation: burst, spikes and silent (Table 3). Differences in RMP or input resistance could not account for different responsiveness. Synaptic currents measured using pipettes filled with potassium gluconate-based solutions were not different. An additional set of voltage-clamp experiments was performed using a caesium-based solution ($n = 14$). The synaptically activated firing pattern of these cells was established in the cell-attached configuration. No differences in synaptic currents measured using the caesium-based solution could account for different responsiveness. In contrast, cells in which bursts were triggered synaptically had a lower firing threshold compared with those that discharged single spikes or did not fire ($P < 0.005$). It is therefore likely that in the subiculum, differences in local responsiveness are related
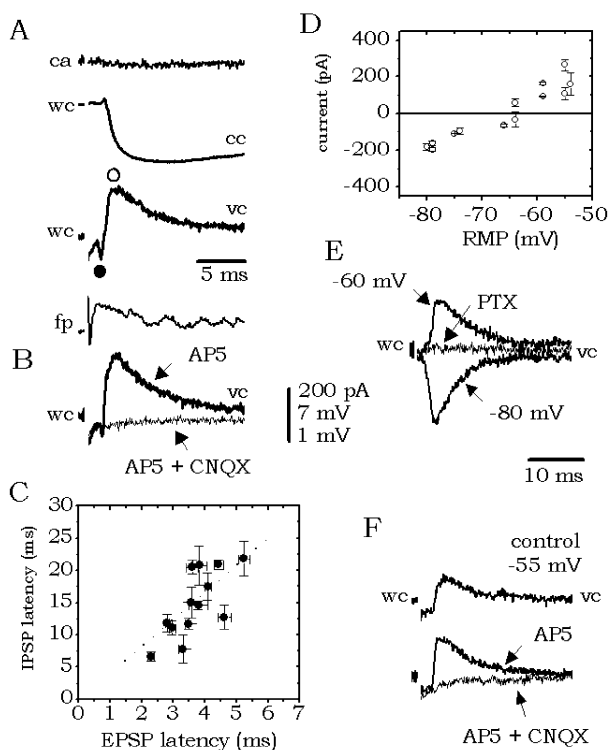
Figure 3. Local GABAergic inhibitory components recorded in some cells in response to local excitation elicited by antidromic activation of projection cells

A, inhibitory responses recorded in current- (cc) and voltage-clamp (vc) mode were typically present as a component of an excitatory/inhibitory sequence. Cells receiving inhibitory responses did not fire in the cell-attached (ca) configuration. *B*, the inhibitory component was abolished by 6-cyano-7-nitroquinoxaline-2,3-dione (CNQX) but not by DL-2-amino-5-phosphonopentanoic acid (AP5). *C*, correlation between the latency of the EPSP peak and the IPSP peak recorded in 13 cells (see ○ and ● in *A*). *D*, reversal potential of the fast inhibitory component calculated from current–voltage curves from four cells (RMP, resting membrane potential). *E*, inhibitory currents were blocked by the GABA$_A$ receptor antagonist picrotoxin (PTX, 100 μM). *F*, in four cells, inhibitory responses were recorded in isolation. They were eliminated by CNQX but not by AP5.

to intrinsic membrane properties and not to synaptic inputs, which were similar in the different electro-physiological groups.

Projection cells receive local inhibition

In addition to purely excitatory responses, some subicular cells received inhibition in response to antidromic stimuli. Inhibitory responses (IPSPs and their corresponding IPSCs) were detected in 25 out of the 85 cells examined, 24 of which were projection cells (including both bursting and RS cells). Inhibitory responses typically consisted of an excitatory–inhibitory sequence recorded both in current- and voltage-clamp modes (Fig. 3*A*, wc traces). In some cells, both a fast and a slow inhibitory component were present. Cells exhibiting inhibitory responses did not fire in the cell-attached configuration at RMP (Fig. 3*A*, ca trace).

The inhibitory synaptic component was abolished by the non-NMDA receptor antagonist CNQX, but not by the NMDA receptor antagonist AP5 ($n = 10$; Fig. 3*B*). This suggests that it could be due to a local innervation of FS interneurons by projection cells since CNQX, but not AP5, blocked glutamatergic excitation. Indeed, the latency of the EPSC and the IPSC peaks (see ● and ○ in Fig. 3*A*) showed a positive correlation ($r = 0.72$ $n = 13$; Fig. 3*C*). In four cells, pure inhibitory events were detected. They had a mean amplitude of 3.8 ± 1.8 mV (186 ± 54 pA) at -50 mV. Their fast component had a reversal potential of -68.1 ± 2.1 mV (Fig. 3*D*) and was blocked by 100 μM PTX (Fig. 3*E*), demonstrating that it is mediated by GABA$_A$ receptors. These pure IPSCs were also blocked by CNQX but not by AP5 (Fig. 3*F*). All of these data suggest that GABAergic pathways are activated locally and that they mediate the inhibitory responses of projection cells.

The possibility that the inhibitory component could be due to a direct activation of GABAergic cells was unlikely,

since: (1) antidromic spikes were not recorded in any of the 16 FS interneurons examined and (2) morphological reconstruction of these cells showed that axon collaterals remained local and did not reach the neighbourhood of the stimulation site (Fig. 4). However, a direct activation of FS cells cannot be completely ruled out (IPSPs exhibiting a faster time to peak of 5–6 ms were recorded in few pyramidal cells). Therefore, I also examined the effect of local application of high [K$^+$] and glutamate on FS interneurons to confirm the hypothesis that the inhibition was mainly recruited by local excitatory circuits.

Figure 5*A* shows the typical experimental configuration used. FS cells were recorded in the cell-attached mode simultaneously with field potential recordings. Once the FS electrophysiological pattern was confirmed, the extracellular electrode was substituted by a patch pipette filled with either 145 mM K$^+$ or 0.5 mM glutamate and connected to the ejection system. Local drops of high [K$^+$] or glutamate were then applied at the same site where antidromic population spikes were recorded. Figure 5*B* shows the synaptic response of a representative FS cell (Fig. 5*C*). Locally applied drops of high [K$^+$] (or glutamate) caused a barrage of EPSPs in FS cells and induced firing at the RMP (Fig. 5*D*, cc traces; $n = 6$ slices examined). Similar to the antidromically activated synaptic events, EPSCs evoked in FS interneurons by drops of high [K$^+$] were blocked by CNQX but not by AP5 (Fig. 5*D*, vc traces).

Effect of local inhibition on the responsiveness of different cell types

In order to evaluate the effect of local inhibition on the responsiveness of different cell types, all experiments on synaptic activation were analysed together. As discussed previously, antidromic stimuli induced an isolated EPSP in 60 out of 85 cells tested. Nearly 75 % of those IB+ cells

Figure 4. Camera lucida reconstruction of three FS interneurons of the subiculum

Axon collaterals are shown in red. The orientation of the cells in the slice is indicated by the axis: FD (fascia dentata), PrS (pre-subiculum).
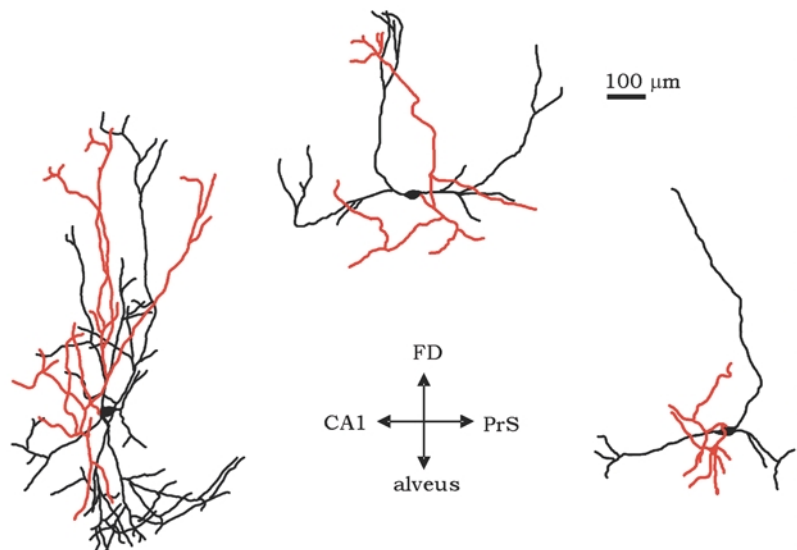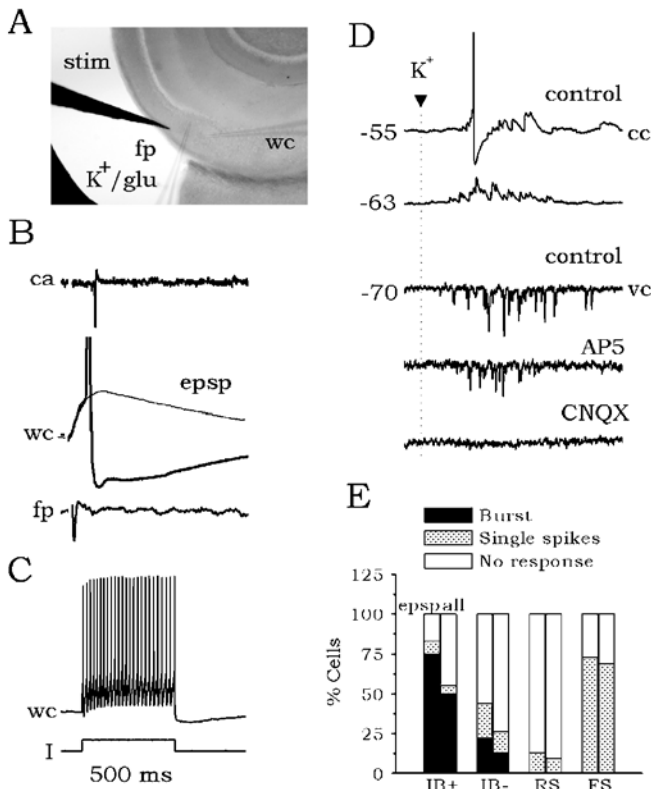
Figure 5. Effect of local microapplication of high [K+]

A, schematic of the experimental design used in the microapplication experiments. The stimulating (stim) and the whole-cell (wc) electrodes were left fixed. Once an FS interneuron was recorded, the field potential electrode (fp) was replaced by a pipette filled with either 145 mM KCl or 0.5 mM glutamate (K+/glu). Local drops of these solutions were then applied. *B*, typical response of an FS cell (*C*) to local excitation elicited by antidromic activation of projection cells. *D*, local drops of high K+ caused a barrage of glutamatergic synaptic events at different membrane potentials as recorded in current- (cc) and voltage-clamp (vc) modes. Similar results were obtained with microapplication of glutamate. The EPSC barrage evoked by microapplication of high K+ was blocked by CNQX but not by AP5. *E*, effect of local inhibition in the responsiveness of distinct cell types to local excitation.

receiving EPSPs fired bursts in cell-attached configuration, whereas ~44 % of IB− cells fired either burst (~22 %) or single spikes (~22 %; Fig. 5*E*, lefthand bars for each group). Less than 15 % of RS cells were synaptically activated, whereas more than 70 % of FS interneurons were induced to fire. When all data (EPSP and IPSP responses, *n* = 85 cells) were analysed together for each group, the proportion of IB+ and IB− cells that fired in response to synaptic activation decreased to ~50 % (Fig. 5*E*, righthand bars for each group). The proportion of

firing cells of the RS and FS groups was not notably affected.

The predominant effect of local inhibition on bursting cells is shown in Fig. 6*A*. No synaptically induced firing was found in the cell-attached configuration. Once in whole-cell mode, a large inhibitory component was recorded. In this electrophysiological cell type, GABAergic inhibition could suppress burst firing (Fig. 6*B*) and in some cases multiple IPSPs and IPSCs were detected (*n* = 4
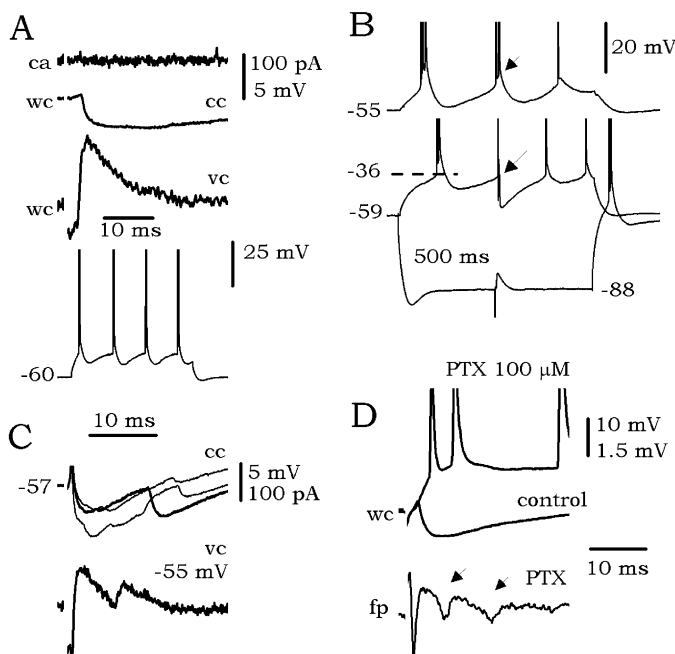
Figure 6. Effect of local inhibition on bursting cells

A, bursting cells (see responses to depolarizing current pulses at the bottom) were prevented from firing in the cell-attached configuration (ca) by large inhibitory components (wc traces). *B*, bursts of firing could be interrupted by evoked IPSPs (arrows). *C*, in some cells, multiple IPSPs and IPSCs were detected. *D*, blockage of GABA_A transmission by 100 μM picrotoxin (PTX) released population epileptiform activity (see arrows in the fp trace).

cells; Fig. 6*C*). When inhibition was blocked by the GABA$_A$ receptor antagonist PTX, bursting in these cells re-emerged and epileptiform population activity was elicited (*n* = 7 isolated subicular slices; Fig. 6*D*, see arrows in the fp trace under PTX).

Effect of local inhibition on subicular bursting

Altogether these results suggest that: (1) IB+ cells (and to a lesser extent IB− cells) are the main contributors to the local excitatory activity of the subiculum and (2) most FS interneurons are innervated locally by projection cells, which contributes to the control of bursting. Qualitative estimates of the impact of this kind of recurrent inhibitory circuit were derived from further experiments based on previous work showing that intrinsic bursts can be antidromically activated in subicular bursting cells (Stewart & Wong, 1993; Stewart, 1997). If most bursting cells were inhibited by a local inhibitory circuit, then antidromically activated bursting should be visible in the field potential on removal of this inhibition (Fig. 7*A*). To this purpose, the glutamate receptor antagonists CNQX and AP5 were used, while GABA$_A$ receptor function was left intact to discriminate from direct inhibition.

In control conditions, antidromic spikes could activate intrinsic bursts in some bursting cells (*n* = 7; Fig. 7*B*, traces ca and wc) but not in the field potential (trace fp). The intrinsic nature of these antidromically activated bursts was confirmed by comparing their waveforms (amplitude, duration) with bursts elicited by depolarizing current pulses (Fig. 7*D*). Antidromically activated bursts in these cells were preserved when glutamatergic excitation was blocked by CNQX and AP5 (Fig. 7*C*, *n* = 7). Interestingly, bursts were detected in the field potential under these conditions (10 out of 13 slices tested; Fig. 7*C*, arrows in trace fp). This suggests that the majority of bursting cells are inhibited, since removing locally activated inhibition resulted in the release of an antidromically activated population burst. This effect was evident in three cells in which IPSPs in control conditions prevented bursts activated by the antidromic spike (Fig. 7*E*, trace wc). Bursts similar to those elicited by depolarizing current pulses (Fig. 7*G*) were released once locally activated inhibition was blocked by CNQX and AP5 (Fig. 7*F*; see arrows in the fp trace). In RS cells, antidromic spikes did not activate bursting (*n* = 3; see cell in Fig. 1*B*).

DISCUSSION

The main results of this study are: (1) bursting cells (mainly strong bursting cells) were the major contributors to a subicular output derived from local activity, since most of them fired in response to local glutamatergic excitation, in contrast to RS cells; (2) FS interneurons were typically excited by local glutamatergic synapses; (3) intrinsic membrane properties, but not the amplitude
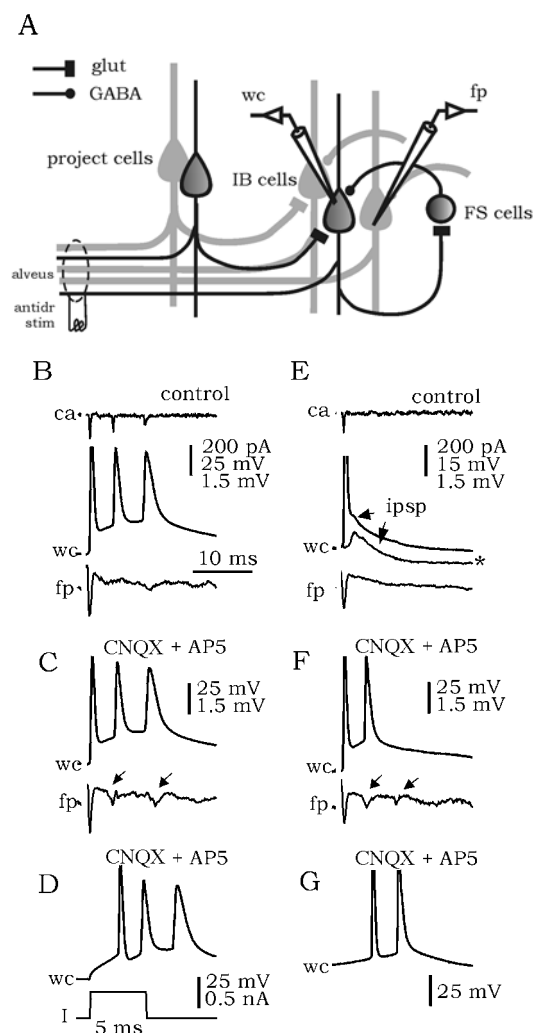
Figure 7. Effect of blockage of locally activated inhibition on the antidromically activated burst

A, schematic of the local excitatory and inhibitory circuits mediating antidromic responses in the subiculum. Antidromic stimulation (antidr stim) of the alveus activates a subpopulation of projection cells (project cells), which in turn excites other projection cells and GABAergic interneurons. If most bursting cells (IB cells) were inhibited by locally activated GABAergic inter-neurons (FS cells), then antidromically activated bursting should be visible in the field potential (fp) on removal of this inhibition by blockers of glutamatergic transmission (glut). *B*, antidromic activation of some bursting cells elicited intrinsic bursts in control conditions in cell-attached (ca) and whole-cell configurations (wc). These bursts were not recorded in the field potential (fp). *C*, blockage of local activation of inhibition by CNQX and AP5 resulted in bursts in the field potential (arrows) suggesting that most bursting cells were inhibited. *D*, intrinsic burst elicited by depolarizing current pulses. Recordings shown in *B–D* are from the same cell. *E*, the effect of local inhibition on antidromically activated bursts was evident in some cells. These bursts were prevented by locally activated IPSPs. See the EPSP/IPSP sequence in the subthreshold curve (*). *F*, blockage of local activation of inhibition released bursting in both wc and fp recordings (arrows in the fp trace). *G*, intrinsic burst elicited by depolarizing current pulses. Recordings shown in *E–G* are from the same cell.

of synaptic currents, determined the responsiveness of different cell types; (4) locally activated firing of FS interneurons contributed to inhibit subicular projection cells; and (5) most bursting cells were inhibited by a local mechanism that prevented burst firing.

Control of subicular output by local inhibition

The subiculum has a strategic position in controlling input and output activity from the hippocampus (Witter, 1993). Its role in memory formation (Zola-Morgan *et al.* 1989; Gabriele *et al.* 1997), spatial encoding (Taube *et al.* 1990) and in the generation of physiological rhythms (Chrobak & Buzsaki, 1996; Stanford *et al.* 1998) has been demonstrated. Furthermore, the hippocampal-subiculum-entorhinal loop has been implicated in temporal lobe epilepsy both in animal studies (Paré *et al.* 1992; Avoli *et al.* 1996; Behr & Heinemann, 1996; Harris & Stewart, 2001) and in human (Schwartzkroin & Hanglund, 1986; Hwa & Avoli, 1992; Cohen *et al.* 2002). In this last case it was shown that alterations of GABAergic inhibition of subicular projection cells were responsible for interictal-like activity (Cohen *et al.* 2002). However, little is known about how the projection cells of the subiculum are controlled by local inhibition.

The projection cells of the subiculum may fire in either bursting or non-bursting modes (Mason, 1993; Stewart & Wong, 1993; Greene & Totterdell, 1997). These two discharge patterns can be divided into different subgroups: weak (IB−) and strong (IB+) bursting (Staff *et al.* 2000; Menendez de la Prida *et al.* 2003) and tonic and adapting RS (Menendez de la Prida *et al.* 2003). Since most RS cells (~87 % of the RS cells examined here) did not respond to local glutamatergic excitation, whereas the majority of bursting cells did (~75 % of IB+ cells and near 45 % of IB− cells), the burst-firing cell group is revealed as the major contributor to a subicular output derived from local activity. Furthermore, pooling together the data from all the projection cell types that receive local excitation (*n* = 45, see Table 3), bursts are the main firing pattern, in contrast to single spikes (although it only represents 29 %, i.e. the majority of projection cells did not respond to local glutamatergic excitation).

Since the first descriptions of intrinsically bursting cells in the subiculum (Mason, 1993; Mattia *et al.* 1993; Stewart & Wong, 1993; Taube, 1993), the bursting nature of its output has been suggested. The large proportion of bursting cells (80–100 %) described in initial studies supported this view. However, subsequent reports indicated a large variability, with a proportion of bursting cells ranging from 50 to 80 % using sharp electrodes (Greene & Totterdell, 1987; Behr *et al.* 1996) and from 30 to 70 % depending on the sampling criteria used in visual patch recordings (Staff *et al.* 2000; Menendez de la Prida *et al.* 2002). Despite this debate, responses of different cell types to local synaptic excitation have not been examined

in detail, and thus qualitative estimates of how bursting and RS cells contribute to the subicular output are not available.

The present data demonstrate a clear contribution of bursting cells to local excitatory activity and to the output firing pattern. However, field potential records of antidromic spikes under control conditions and under conditions of blockage of locally activated inhibition suggest that most bursting subicular cells are subject to an inhibitory control. This could explain why the subiculum acts as an epileptogenic structure when GABAergic inhibition is removed (Miles & Wong, 1987; Harris & Stewart, 2001; Cohen *et al.* 2002; Menendez de la Prida & Pozo, 2002). This local inhibitory control of projection cells could also be the cellular mechanism supporting the feedforward inhibition of subicular firing in response to afferent stimulation (Finch & Babb, 1980; Colino & De Molina, 1986; Finch *et al.* 1988).

Anatomical support for local inhibition in the subiculum is provided by the presence of both glutamatergic and GABAergic cells that are densely connected. The intrinsic synaptic organization of the subiculum is less well under-stood than that of the hippocampus. Indirect information from both electrophysiological and morphological studies has helped to draw a picture of the connectivity patterns. Bursting and RS cells are known to make numerous local synaptic contacts in the subicular cell layer and in the apical dendritic region (Köhler, 1986; Witter, 1993; Harris *et al.* 2001). Based on this data, a columnar and laminar architecture has been suggested (Funahashi & Stewart, 1997; Naber & Witter, 1998; Harris *et al.* 2001). Nevertheless, the absence of direct information on synaptic interactions means that the complete microanatomical picture is missing. For example, the divergence/convergence ratio of inhibitory and excitatory subicular connections remains unknown, and there are no quantitative estimates of synaptic connectivity between distinct cell types.

The present data show no differences in excitatory synaptic currents impinging on the different cell types. For pyramid-to-pyramid interactions, conductances were in the range of 5–17 nS, whereas a value of 3–8 nS was encountered for pyramid-to-interneuron connections (data estimated from current–voltage curves for synaptic currents, not shown). Inhibitory conductances in projection cells were in the range of 10–16 nS. These values are comparable to those reported for hippocampal pyramidal cells, suggesting that the two structures possess similarities in local connectivity (Traub & Miles, 1991). Further experiments are needed to understand the micro-anatomical organization of the subiculum underlying the local inhibitory pathways and to identify similarities and differences to the CA3 and CA1 regions of the hippocampus.

Strong and weak subicular bursting cells: a functional separation

Another important result is the different synaptic responses of cells demonstrating strong and weak intrinsic bursts discharges. These two cell types were first separated by electrophysiological characterization of their intrinsic firing patterns (Staff *et al.* 2000), and subsequent work suggests that differences in low- and high-threshold calcium currents are responsible (Jung *et al.* 2001; Menendez de la Prida *et al.* 2003). The present data show that IB+ cells typically generate a burst of action potentials, whilst more than 50 % of IB− neurons remain silent in response to similar synaptic stimuli. This observation was made in both the cell-attached and whole-cell configurations, suggesting that it did not depend on cell dialysis.

According to a randomly sampled population of neurons, bursting cells of the subiculum represent ~30 % of the total (Menendez de la Prida *et al.* 2002), of which half are of the IB+ type. Since most IB+ cells that receive local excitation fire bursts, in contrast to a lesser proportion of IB− cells, the IB+ cells seem likely to represent the major source of subicular discharges. *In vitro* (Harris & Stewart, 2001) and *in vivo* studies (Finch *et al.* 1988; Gigg *et al.* 2000) have demonstrated that bursting cells are spontaneously active. They participate in both specific physiological rhythms (Stanford *et al.* 1998) and in pathological activity such as epilepsy (Harris & Stewart, 2001). The functional differences between IB+ and IB− cells suggest that further explorations of possible distinct roles in the generation of population activity would be fruitful. Indeed, it would be very important to explore further the relationship between intrinsic currents, such as sodium-persistent and calcium currents, in IB+ and IB− cells determining different synaptic responsiveness (Jung *et al.* 2001).

Functional implication for the operation of subicular circuitry

Inhibition may be modulated by oscillatory activity in specific frequency bands (Toth *et al.* 1997; Bracci *et al.* 2001), by homeostatic alterations in the HCO_3^-/CO_2 equilibrium (Staley *et al.* 1995; Staley & Proctor, 1999) or by presynaptic and postsynaptic mechanisms (Freund *et al.* 1990; Rodriguez-Moreno & Lerma, 1998; Gulyás *et al.* 1999). Furthermore, reactive plasticity caused by deafferentation, for example, could shift GABAergic function from hyperpolarizing to depolarizing, resulting in network disinhibition (Van den Pol *et al.* 1996). The present results suggest that the subiculum would be especially susceptible to all of these changes. Indeed, recent evidence from the human epileptic subiculum suggests specific alterations of the inhibitory control, presumably associated with sclerosis of the CA1 region (Cohen *et al.* 2002). This remodelling of the inhibitory control could run in parallel with an upregulation of intrinsic bursting,

as demonstrated recently in pilocarpine-treated rats (Wellmer *et al.* 2002). It is therefore important to understand the cellular basis of the inhibitory control of bursting, which endows the subiculum with an intrinsic mechanism able to modulate its output under both normal and pathological situations.

REFERENCES

Alger BE & Nicoll RA (1982). Feed-forward dendritic inhibition in rat hippocampal cells studied *in vitro*. *J Physiol* **328**, 105–123.

Avoli M, Barbarosie M, Lücke A, Nagao T, Lopantsev V & Köhling R (1996). Synchronous GABA-mediated potentials and epileptiform discharges in the rat limbic system *in vitro*. *J Neurosci* **16**, 3912–3924.

Behr J, Empson RM, Schmitz D, Gloveli T & Heinemann U (1996). Electrophysiological properties of rat subicular neurons *in vitro*. *Neurosci Lett* **220**, 41–44.

Behr J, Gloveli T & Heinemann U (1998). The perforant path projection from the medial entorhinal cortex layer III to the subiculum in the rat combined hippocampal-entorhinal cortex slice. *Eur J Neurosci* **10**, 1011–1018.

Behr J & Heinemann U (1996). Low Mg^{2+} induced epileptiform activity in the subiculum before and after disconnection from rat hippocampal and entorhinal cortex slices. *Neurosci Lett* **205**, 25–28.

Bracci E, Vreugdenhil M, Hack SP & Jefferys JGR (2001). Dynamic modulation of excitation and inhibition during stimulation at gamma and beta frequencies in the CA1 hippocampal region. *J Neurophysiol* **85**, 2412–2422.

Buzsaki G (1984). Feed-forward inhibition in the hippocampal formation. *Prog Neurobiol* **22**, 131–153.

Christian EP & Dudek FE (1988). Characteristics of local excitatory circuits studied with glutamate microapplication in the CA3 area of the rat hippocampal slices. *J Neurophysiol* **59**, 90–109.

Chrobak JJ & Buzsaki G (1996). High-frequency oscillations in the output networks of the hippocampal-entorhinal axis of the freely behaving rat. *J Neurosci* **16**, 3056–3066.

Cohen I, Navarro V, Clemenceau S, Baulac M & Miles R (2002). On the origin of interictal activity in human temporal lobe epilepsy *in vitro*. *Science* **298**, 1418–1421.

Colino A & De Molina FF (1986). Inhibitory response in entorhinal and subicular cortices after electrical stimulation of the lateral and basolateral amygdala of the rat. *Brain Res* **378**, 416–419.

Finch DM & Babb TL (1980). Inhibition in subicular and entorhinal principal neurons in response to electrical stimulation of the fornix and hippocampus. *Brain Res* **196**, 89–98.

Finch DM, Nowlin NL & Babb TL (1983). Demonstration of axonal projections of neurons in the rat hippocampus and subiculum by intracellular injection of HRP. *Brain Res* **271**, 201–216.

Finch DM, Tan AM & Isokawa-Akesson M (1988). Feedforward inhibition of the rat entorhinal cortex and subicular complex. *J Neurosci* **8**, 2213–2226.

Freund TF, Gulyás AI, Acsady L, Görcs T & Toth K (1990). Serotoninergic control of the hippocampus via local inhibitory interneurons. *Proc Natl Acad Sci U S A* **87**, 8501–8505.

Funahashi M & Stewart M (1997). Presubicular and parasubicular cortical neurons of the rat: functional separation of deep and superficial neurons *in vitro*. *J Physiol* **501**, 387–403.

Gabriele JDE, Brewer JB, Desmond JE & Glover GH (1997). Separate neural bases of two fundamental memory processes in the human medial temporal lobe. *Science* **276**, 264–266.

Gigg J, Finch DM & O'Mara SM (2000). Responses of rat subicular neurons to convergent stimulation of lateral entorhinal cortex and CA1 *in vivo*. *Brain Res* **884**, 35–50.

Greene JRT & Totterdell S (1997). Morphology and distribution of electrophysiologically defined classes of pyramidal and nonpyramidal neurons in rat ventral subiculum *in vitro*. *J Comp Neurol* **380**, 395–408.

Gulyás AI, Acsady L & Freund TF (1999). Structural basis of the cholinergic and serotoninergic modulation of GABAergic neurons in the hippocampus. *Neurochem Int* **34**, 359–372.

Harris E & Stewart M (2001). Intrinsic connectivity of the rat subiculum: II. Properties of synchronous spontaneous activity and a demonstration of multiple generator regions. *J Comp Neurol* **436**, 506–518.

Harris E, Witter MP, Weinstein G & Stewart M (2001). Intrinsic connectivity of the rat subiculum: I. Dendritic morphology and patterns of axonal arborization by pyramidal neurons. *J Comp Neurol* **436**, 490–505.

Hwa GG & Avoli M (1992). Excitatory synaptic transmission mediated by NMDA and non-NMDA receptors in the superficial/middle layers of the epileptogenic human neocortex maintained *in vitro*. *Neurosci Lett* **143**, 83–86.

Ishizuka N (2001). Laminar organization of the pyramidal cell layer of the subiculum in the rat. *J Comp Neurol* **435**, 89–110.

Jung H, Staff NP & Spruston N (2001). Action potential bursting in subicular pyramidal neurons is driven by a calcium tail current. *J Neurosci* **21**, 3312–3321.

Kawaguchi Y & Hama K (1987). Fast-spiking non-pyramidal cells in the hippocampal CA3 region, dentate gyrus and subiculum of rats. *Brain Res* **425**, 351–355.

Köhler C (1986). Intrinsic projections of the retrohippocampal region in the rat brain: I The subicular complex. *J Comp Neurol* **236**, 504–522.

Mason A (1993). Electrophysiology and burst-firing of rat subicular pyramidal neurons *in vitro*: a comparison with area CA1. *Brain Res* **600**, 174–178.

Mattia D, Hwa GGC & Avoli M (1993). Membrane properties of rat subicular neurons *in vitro*. *J Neurophysiol* **70**, 1244–1248.

Menendez de la Prida L & Pozo MA (2002). Excitatory and inhibitory control of epileptiform discharges in combined hippocampal/entorhinal cortical slices. *Brain Res* **940**, 27–35.

Menendez de la Prida L, Suarez F & Pozo MA (2002). The effect of different morphological sampling criteria on the fraction of bursting cells recorded in the rat subiculum *in vitro*. *Neurosci Lett* **322**, 49–52.

Menendez de la Prida L, Suarez F & Pozo MA (2003). Electrophysiological and morphological diversity of neurons from the rat subicular complex *in vitro*. *Hippocampus* (in the Press).

Miles R & Wong RKS (1986). Excitatory synaptic interactions between CA3 neurones in the guinea-pig hippocampus. *J Physiol* **373**, 397–418.

Miles R & Wong RKS (1987). Inhibitory control of local excitatory circuits in the guinea-pig hippocampus. *J Physiol* **388**, 611–629.

Naber PA & Witter MP (1998). Subicular efferents are organized mostly as parallel projections: a double-labeling, retrograde-tracing study in the rat. *J Comp Neurol* **393**, 284–297.

Paré D, Decurtis M & Llinás R (1992). Role of the hippocampal-entorhinal loop in temporal lobe epilepsy: extra- and intracellular study in the isolated guinea pig brain *in vitro*. *J Neurosci* **12**, 1867–1881.

Rodriguez-Moreno A & Lerma J (1998). Kainate receptor modulation of GABA release involves a metabotropic function. *Neuron* **20**, 1211–8.

Schwartzkroin PA & Haglund MM (1986). Spontaneous rhythmic synchronous activity in epileptic human and normal monkey temporal lobe. *Epilepsia* **27**, 523–533.

Staff NP, Jung H, Thiagarajan T, Yao M & Spruston N (2000). Resting and active properties of pyramidal neurons in subiculum and CA1 of rat hippocampus. *J Neurophysiol* **84**, 2398–2400.

Staley KJ & Proctor WR (1999). Modulation of mammalian dendritic GABA(a) receptor function by the kinetics of the Cl$^-$ and HCO$_3^-$ transport. *J Physiol* **519**, 693–712.

Staley KJ, Soldo BL & Proctor WR (1995). Ionic mechanisms of neuronal excitation by inhibitory GABAa receptors. *Science* **269**, 977–981.

Stanford IM, Traub RD & Jefferys JGR (1998). Limbic gamma rhythms. II. Synaptic and intrinsic mechanisms underlying spike doublets in oscillating subicular neurons. *J Neurophysiol* **80**, 162–171.

Stewart M (1997). Antidromic and orthodromic responses by subicular neurons in rat brain slices. *Brain Res* **769**, 71–85.

Stewart M & Wong RK (1993). Intrinsic properties and evoked responses of guinea-pig subicular neurons *in vitro*. *J Neurophysiol* **70**, 232–245.

Taube JS (1993). Electrophysiological properties of neurons in the rat subiculum *in vitro*. *Exp Brain Res* **96**, 304–318.

Taube JS, Muller RU & Ranck JB Jr (1990). Head-direction cells recorded from the postsubiculum in freely moving rats. I. Description and quantitative analysis. *J Neurosci* **10**, 420–435.

Traub RD & Miles R (1991). *Neuronal Networks of the Hippocampus*. Cambridge University Press, Cambridge

Toth K, Freund TF & Miles R (1997). Disinhibition of rat hippocampal pyramidal cells by GABAergic afferents from the septum. *J Physiol* **500**, 463–474.

Van den Pol AN, Obrietan K & Chen G (1996). Excitatory actions of GABA after neuronal trauma. *J Neurosci* **16**, 4283–4292.

Van Groen T & Lopes da Silva FH (1986). Organization of the reciprocal connections between the subiculum and the entorhinal cortex in the cat: II. An electrophysiology study. *J Comp Neurol* **251**, 111–120.

Wellmer J, Su H, Beck H & Yaari Y (2002). Long-lasting modification of intrinsic discharge properties in subicular neurons following status epilepticus. *Eur J Neurosci* **16**, 259–266.

Witter MP (1993). Organization of the entorhinal-hippocampal system: a review of current anatomical data. *Hippocampus* **3**, 33–44.

Zola-Morgan S, Squire LR, Amaral DG & Suzuki WA (1989). Lesions of perirhinal and parahippocampal cortex that spare the amygdala and hippocampal formation produce severe memory impairment. *J Neurophysiol* **9**, 4355–4370.